

Doubled Moiré Flat Bands in Double-twisted Few Layer Graphite

Zhen Ma,¹ Shuai Li,¹ Ming Lu,^{2,3} Dong-Hui Xu,⁴ Jin-Hua Gao,^{1,*} and X. C. Xie^{3,5,6}

¹*School of Physics and Wuhan National High Magnetic Field Center, Huazhong University of Science and Technology, Wuhan 430074, China*

²*Beijing Academy of Quantum Information Sciences, Beijing 100193, China*

³*International Center for Quantum Materials, School of Physics, Peking University, Beijing 100871, China*

⁴*Department of Physics, Hubei University, Wuhan 430062, China*

⁵*Collaborative Innovation Center of Quantum Matter, Beijing 100871, China*

⁶*CAS Center for Excellence in Topological Quantum Computation, University of Chinese Academy of Sciences, Beijing 100190, China*

We study the electronic structure of a double-twisted few layer graphite (DTFLG), which consists of three few layer graphite (FLG), *i.e.* ABA-stacked graphene multilayer, stacked with two twist angles. We consider two categories of DTFLG, alternately twisted case and chirally twisted one, according to the rotation direction of the two twist angles. We show that, once the middle FLG of DTFLG is not thinner than trilayer, both kinds of DTFLG can remarkably host two pairs of degenerate moiré flat bands (MFBs) at E_f , twice that of the magic angle twisted bilayer graphene (TBG). The doubled MFBs of DTFLG lead to doubled DOS at E_f , which implies much stronger correlation effects than the TBG. The degeneracy of MFBs can be lifted by a perpendicular electric field, and the isolated MFBs have nonzero valley Chern number. We also reveal the peculiar wave function patterns of the MFBs in the DTFLG. Our results establish a new family of moiré systems that have the much larger DOS at E_f , and thus possible much stronger correlation effects.

Introduction.—Twisted bilayer graphene (TBG) host a pair of moiré flat bands (MFBs) at the so-called magic angle (per valley per spin) [1–3]. The giant density of states (DOS) and quenched kinetic energy of the MFBs are especially conducive to interaction-driven states. Mott-like insulating state and unconventional superconductivity have already been observed in TBG, which has drawn great research interest very recently[4–11]. Actually, MFB is a general phenomenon of moiré heterostructures (MHSs). It exists in many other similar MHSs, such as twisted double bilayer graphene [12–23], twisted trilayer graphene [24–32], trilayer graphene on boron nitride[33–35], twisted few layer graphite[36, 37], *etc.* Interestingly, the MFBs in some of these MHSs are topological nontrivial[12–15, 24, 38, 39], and topological phenomena, *e.g.* intrinsic quantum anomalous hall effect[40–42], can arise due to these topological MFBs. Very recently, MFBs in multi-twisted MHSs also have been studied [43–55].

In general, the larger DOS is, the stronger electronic correlation is. Thus, a fascinating question is whether it is possible to further enhance the DOS of the moiré flat band systems, so that the correlation phenomena in MHSs can be more evident with a higher transition temperature. At first glance, it is hardly possible since that a flat band already reaches the DOS maximum of a single band. Note that, in nearly all the MSHs reported so far, we can get at most a pair of MFBs at the Fermi level E_f .

In this work, we report a new MHS family, *double-twisted few layer graphite* (DTFLG), which remarkably can host *two* pairs of degenerate MFBs at the Fermi level, *i.e.* twice as much as that in TBG. Since the number of flat bands has doubled, the DOS of the DTFLG can be twice that of the magic angle TBG, which im-

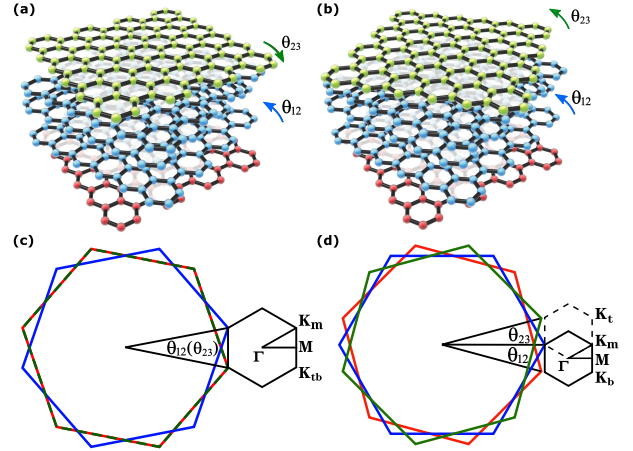


FIG. 1. (a) is the schematic of the (1+3+1)-aDTFLG and (c) is the corresponding moiré BZ. (b) is the schematic of the (1+3+1)-cDTFLG and (d) is the corresponding moiré BZ. θ_{12} and θ_{23} are the two twist angles. Red, blue and green represent the bottom, middle and top vdW layer, respectively.

plies much stronger correlation effects and possible higher transition temperature than the magic angle TBG. DTFLG is a sandwich-like MHS, which consists of three few layer graphite (FLG), *i.e.* ABA-stacked graphene multilayer, stacked with two twist angles. We show that once the sandwiched middle FLG is not thinner than trilayer, no matter the DTFLG is alternately [43] or chirally [45] twisted, the DTFLG always have two pairs of degenerate MFBs at certain magic angle. Meanwhile, different band structures of MFBs, *i.e.* isolated flat bands or coexisting with other dispersive bands, can be achieved by choosing different stacking arrangements of DTFLG. Such MFBs

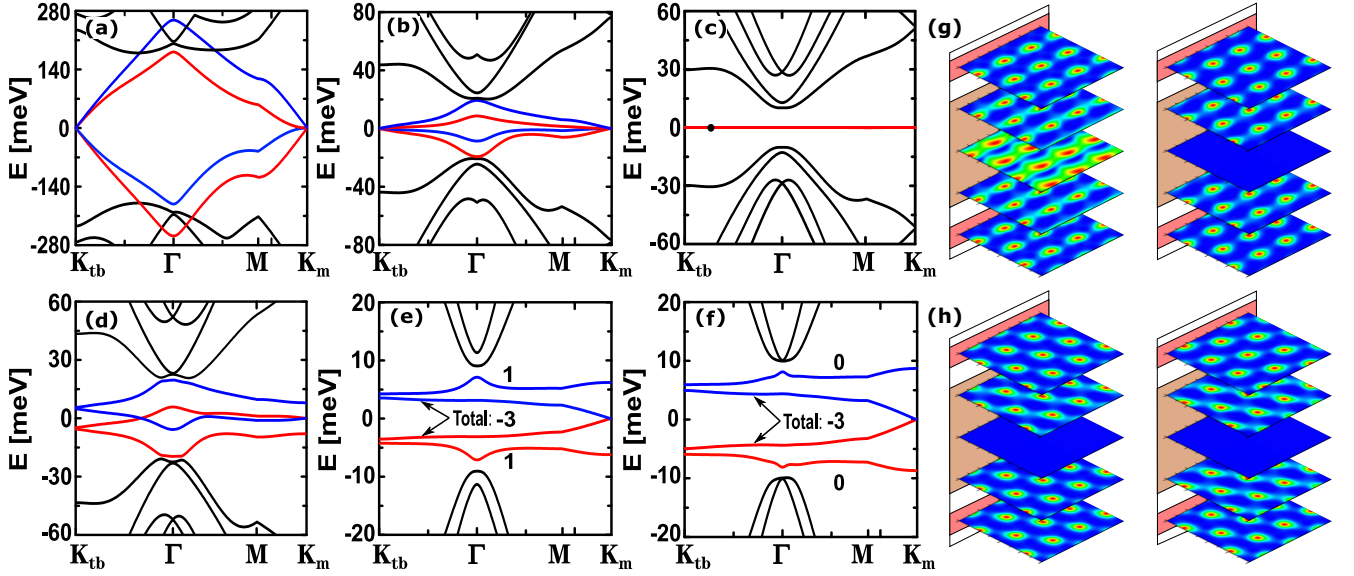


FIG. 2. (a-f) are the moiré band structure of a (1+3+1)-aDTFLG. The parameters are: (a) $\theta = 2.88^\circ$, (b) $\theta = 1.25^\circ$, (c) $\theta = 1.08^\circ$, (d) $\theta = 1.25^\circ$ and $V = 5$ meV, (e) $\theta = 1.08^\circ$ and $V = 5$ meV, (f) $\theta = 1.08^\circ$ and $V = 7$ meV. (g) and (h) show the flat band wave function distribution in each graphene monolayer, which correspond to the k state marked (black dot) in (c). (g) is for 2nd MFB of the total 4 MFBs from bottom to up, and (f) is for the top MFB. Left (right) column is for A (B) sublattice of each graphene monolayer. The parameters: $\omega_{AA} = 0.0797$ eV, $\omega_{AB} = 0.0975$ eV.

in DTFLG are topological nontrivial and can be further adjusted by a perpendicular electric field. In experiment, the double twisted MHS has already been realized in recent experiments[54, 55], so that the fabrication of DTFLG should be not too challenging. Our study indicates that the DTFLG is a promising moiré platform that can realize stronger correlation effects, and double twist can give rise to unique flat physics that is absent in single-twist MHSs like TBG.

Structure of DTFLG.—A general (M+N+P)-DTFLG is composed of three van der Waals (vdW) layers twisted relative to the adjacent layer, where each vdW layer is a FLG. Here, M, N and P represent the layer number of the bottom (1st vdW layer), middle (2nd vdW layer) and top FLG (3rd vdW layer), respectively. Fig. 1 shows the typical example of (1+3+1)-DTFLG, in which we use θ_{12} (θ_{23}) to denote the twist angle between the middle and bottom (top and middle) vdW layers. Note that, according to sign of the two twist angles θ_{12} and θ_{23} , we have two kinds of DTFLG: (1) alternately twisted DTFLG (aDTFLG) in Fig. 1 (a) with $\theta_{12} = -\theta_{23}$ [43]; (2) chirally twisted DTFLG (cDTFLG) in Fig. 1 (b) with $\theta_{12} = \theta_{23}$ [45]. Here, we always assume that $\theta \equiv |\theta_{12}| = |\theta_{23}|$, since otherwise the supercell of DTFLG does not exist. Note that, when $\theta = 0$, both (1+3+1)-aDTFLG and (1+3+1)-cDTFLG return to a AABAA-stacked graphene quintuple-layer. The moiré Brillouin zones (BZ) of the aDTFLG and cDTFLG are given in Fig. 1 (c) and (d), respectively.

Not all the DTFLG has two pairs of MFBs. The key requirement is that $N \geq 3$, *i.e.* the middle FLG

at least should be a ABA-stacked graphene trilayer. So, the (1+3+1)-DTFLG is the simplest case, which has two degenerate MFBs. The reason is because the layer number of FLG determines the number of energy bands at E_f . A N-layer FLG has N (N-1) parabolic bands when N is even (odd) near the E_f , together with an additional pair of linear bands if N is odd. Therefore, ABA-trilayer graphene has two pairs of energy bands at E_f . Interestingly, when such two pair of energy bands are coupled with the top and bottom vdW layers via moiré interlayer hopping, they are simultaneously flattened at certain magic angle, so that we finally get two pair of degenerate MFBs at zero energy. This novel phenomenon exist in all the DTFLG with $N \geq 3$ (both alternately twist and chirally twist cases), which is the main result of this work.

Continuum model.—We use continuum model to calculate the moiré band structure of the DTFLG. Both aDTFLG and cDTFLG can be described by an unified Hamiltonian, which reads as a 3×3 block matrix

$$H_{\text{DTFLG}} = \begin{pmatrix} H_1(k_1) & T_{12}(r) & 0 \\ T_{12}^\dagger(r) & H_2(k_2) & T_{23}(r) \\ 0 & T_{23}^\dagger(r) & H_3(k_3) \end{pmatrix}. \quad (1)$$

The diagonal matrices are the tight-binding Hamiltonian of FLG in the Bloch wave basis, and the off-diagonal matrices describe moiré interlayer hopping. For example, $H_1(k_1)$ describes the bottom vdW layer, *i.e.* the M-layer FLG in a general (M+N+P)-DTFLG, which is a $2M \times 2M$ matrix. $k_1 = k - K_1$, where k is the momentum relative to the Γ point and K_1 is the Dirac point of

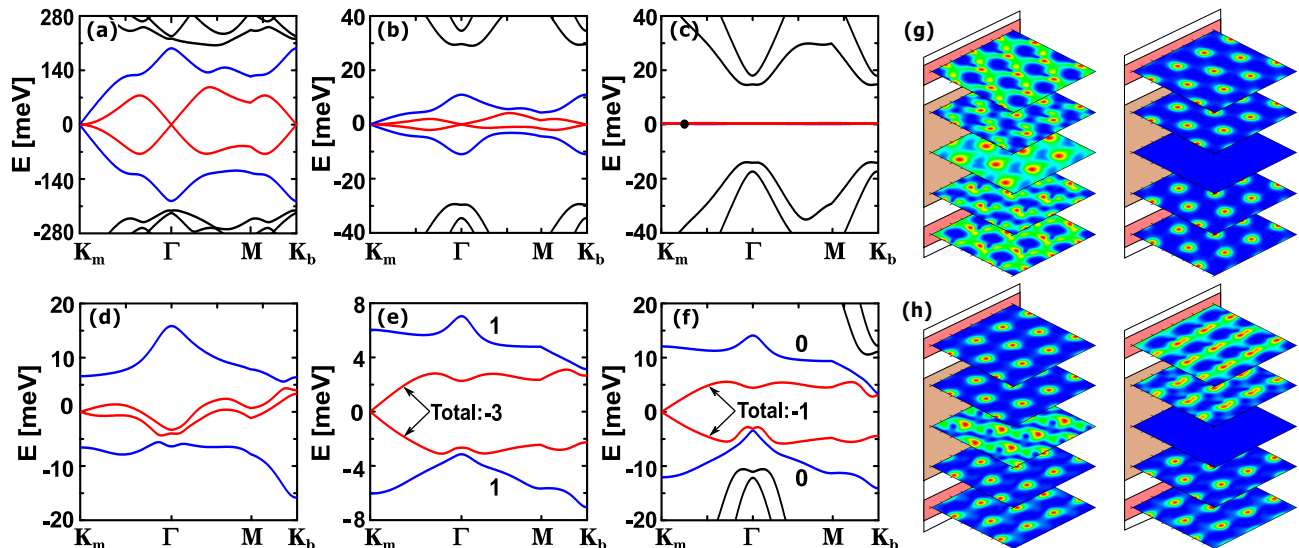


FIG. 3. (a-f) are the moiré band structure of a (1+3+1)-cDTFLG. The parameters are: (a) $\theta = 2.88^\circ$, (b) $\theta = 1.25^\circ$, (c) $\theta = 1.08^\circ$, (d) $\theta = 1.25^\circ$ and $V = 5$ meV, (e) $\theta = 1.08^\circ$ and $V = 5$ meV, (f) $\theta = 1.08^\circ$ and $V = 10$ meV. (g) and (h) show the flat band wave function distribution in each graphene monolayer, which correspond to the k state marked (black dot) in (c). (g) is for 2nd MFB of the total 4 MFBs from bottom to up, and (f) is for the top MFB. Left (right) column is for A (B) sublattice of each graphene monolayer. The parameters: $\omega_{AA} = 0.0797$ eV, $\omega_{AB} = 0.0975$ eV.

the bottom vdW layer. $H_2(k_2)$ and $H_3(k_3)$ are given in the same way, which describe the middle and top vdW layer, respectively. The moiré interlayer hopping between adjacent vdW layers are $T_{ij}(r) = \sum_{n=0,1,2} T_{ij}^n \cdot e^{-iq_n \cdot r}$, where $q_n = 2k_D \sin(\frac{\theta}{2}) \exp(i\frac{2n\pi}{3})$ and k_D is the magnitude of the BZ corner wave vector of a single vdW layer. And,

$$T_{ij}^n = I_{ij} \otimes \begin{pmatrix} \omega_{AA} & \omega_{AB}e^{i\phi_n} \\ \omega_{AB}e^{-i\phi_n} & \omega_{AA} \end{pmatrix}. \quad (2)$$

Here, I_{ij} is a matrix with only one nonzero matrix element. For instance, in a (M+N+P)-DTFLG, the only nonzero matrix element of I_{12} is $I_{12}(M, N) = 1$. $\phi_n = \text{sign}(\theta_{ij})\frac{2n\pi}{3}$, in which the sign of θ_{ij} denotes the rotation direction. Note that the above formulas are only valid for the cases with a small twist angle θ .

Flat bands of (1+3+1)-aDTFLG.—We first discuss the moiré band structure of the (1+3+1)-aDTFLG, as an example of the aDTFLG. In Fig. 2 (a), we plot the moiré band with a large angle $\theta = 2.88^\circ$. Here, K_m belongs to the middle FLG (ABA-trilayer), and K_{tb} is from the top and bottom FLGs (graphene monolayers). Without moiré interlayer hopping, near the K_m , there are a pair of linear bands and a pair of parabolic bands from the middle ABA-trilayer. Meanwhile, the top and bottom graphene monolayer each provides one pairs of linear bands at K_{tb} with the same Fermi velocity. At large θ , we can see that the moiré interlayer hopping hybridizes the two pairs of bands at K_m and K_{tb} , and finally two pairs of moiré bands are formed near the charge neutrality point, see the blue and red solid lines in Fig. 2 (a).

Interestingly, due to the moiré interlayer hopping, the Fermi velocity of the two pairs of linear bands at K_{tb} becomes different, so that they are not degenerate any more. Decreasing θ , the band width of the four moiré bands are narrowed. Around $\theta = 1.25^\circ$, the two pair of central moiré bands are separated from other high energy bands and a small gap appears, see Fig. 2 (b). Remarkably, when θ approaches 1.08° , the two pairs of moiré bands becomes complete flat (bandwidth is smaller than 1 meV) almost at the same time, see Fig. 2 (c). These four MFBs at zero energy are separated from other high energy bands by a gap about 10 meV.

We emphasize that the double twist structure and the multi-bands feature of the FLG ($N \geq 3$) are the two indispensable requirements for obtaining the two pairs MFBs. Here, we give two counterexamples. One is the (1+1+1)-aDTFLG (*i.e.* double-twisted trilayer graphene), which do not satisfy the demand for $N \geq 3$. Since the middle vdW layer just has two bands at E_f , the (1+1+1)-aDTFLG can only host a pair of MFBs, coexisting with a pair of linear bands[43]. The other is the (ABA+ABA)-type twisted FLG, which is a single twist MHS. Though it also has four bands near E_f at the two inequivalent Dirac points of the moiré BZ, a single twist can only induce one pair of MFBs at zero energy as well [36]. Our calculations indicate that all the DTFLG with $N \geq 3$, meeting these two requirements above, have two pairs of degenerate MFBs at the magic angle about 1.08° , the magic angle of which is the same as that of TBG but different from that of the double twisted trilayer graphene (about 1.5°)[43].

We can use a perpendicular electric field to lift the degeneracy of the flat bands. Note that flat band states at K_{tb} point come from the top and bottom vdW layers. If a perpendicular electric field is applied, each vdW layer in the DTFLG feels different potential, and thus the degeneracy of the flat bands is lifted. Here, we use the potential difference between the adjacent layers V to represent the electric field. In Fig. 2 (d), we apply an electric field $V = 5$ meV ($\theta = 2.88^\circ$). We see that, at K_{tb} , two moiré bands (blue lines) are shifted upwards, which implies that they are mainly from the bottom graphene monolayer. Similarly, the other two bands shifted downwards (red lines) are from the top layer. At K_m , the four bands near E_f are from the middle ABA-trilayer. Under the electric field, the two outer bands are gapped, while the inner two are still degenerate at K_m . Such band behaviours under electric field is in agreement with that of a ABA-trilayer. Similar phenomenon can be observed at the magic angle, see Fig. 2 (e) and (f).

The moiré flat bands of the (1+3+1)-aDTFLG are topological nontrivial. Without electric field, the valley Chern number of the moiré flat bands are not well-defined, since the moiré flat bands are all degenerate at zero energy. However, electric field can lift all the degeneracy of the four MFBs, except for the degeneracy of the middle two bands at K_m point, see Fig. 2 (e). Note that there is a tiny gap between the top (bottom) two MFBs at K_{tb} , which can be further enlarged by increasing the electric field, see Fig. 2 (f). Thus, the outer two MFBs are isolated. We then calculate the valley Chern number of the two isolated MFBs with the standard formula. When $V = 5$ meV, the valley Chern numbers of the two moiré flat bands are 1, see Fig. 2 (e). And, though the middle two MFBs are still connected, the total valley Chern number of the two bands are 3, also a nonzero value. Such topological nontrivial MFBs indicate that, once the valley degeneracy is lifted by the symmetry broken, orbital magnetization, quantum anomalous hall effects and other valley Chern number related topological phenomena may occur, just like that in other topological moiré systems. Meanwhile, the interplay between correlation and band topology in DTFLG should be different from former moiré systems, because of its multi-flat-band feature.

The valley Chern number can be changed by adjusting the electric field. For example, if we apply a larger electric field $V = 7$ meV, a band cross can happen between the top (bottom) MFB and higher excited bands. As shown in Fig. 2 (f), a change of valley Chern number from 1 to 0 occurs simultaneously in the outer two isolated MFBs.

Typical wave functions of the MFBs in (1+3+1)-aDTFLG are shown in Fig. 2 (g) and (h), which corresponds to the denoted k point in Fig. 2 (c). Fig. 2 (g) is for the 2nd MFB from bottom to top, where the left (right) column is the wave function at sublattice A (B)

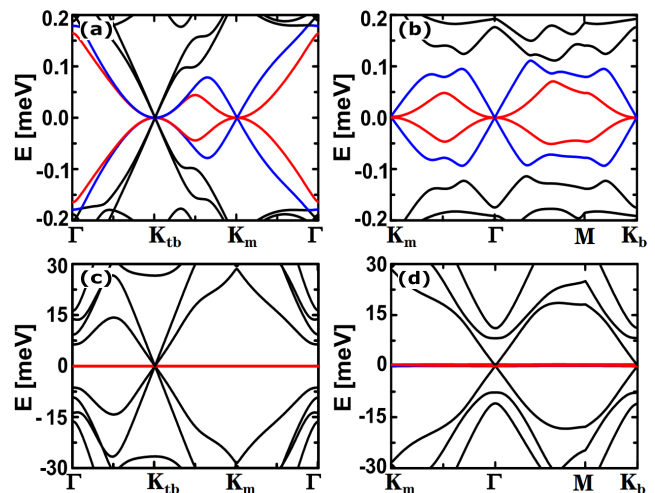


FIG. 4. Moiré band structures of the (3+3+3)-DTFLG. (a) and (c) are for the alternately twisted case with $\theta = 2.88^\circ$ and $\theta = 1.08^\circ$, respectively. (b) and (d) are for the chirally twisted case with $\theta = 2.88^\circ$ and $\theta = 1.08^\circ$, respectively.

in each graphene monolayer. Interestingly, we find that over 75% of the wave function lie in the sublattice A of the middle graphene monolayer, while that is zero in the sublattice B of the middle graphene monolayer, see Fig. 2 (g). Fig. 2 (h) is for the top MFB, where the wave function is zero at the middle graphene monolayer. The wave function of the bottom MFB is like the top one, while that of the middle two MFBs are similar.

Flat bands in (1+3+1)-cDTFLG.—We then discuss the moiré band structures of the (1+3+1)-cDTFLG. The moiré BZ of the cDTFLG is different from that of aDTFLG. As shown in Fig. 1 (d). The Dirac cones at zero energy of the top, middle and bottom vdW layers are attached to the Γ , K_m , and K_b points, respectively. Electronic states around the three Dirac points are coupled by the moiré interlayer hopping to form the moiré band structures at E_f .

In the chirally twisted case, (1+3+1)-cDTFLG also has fundamentally different moiré band structure from that of (1+1+1)-cDTFLG (*i.e.* a double twisted trilayer graphene), though their moiré BZs are similar. The (1+1+1)-cDTFLG is a perfect metal, where the moiré bands are always connected and gapless at all energy. And it does not have perfect flat bands. In contrast, as shown in Fig. 3, the (1+3+1)-cDTFLG has four moiré bands at zero energy, gapped from other excited bands. Fig. 3 (a) gives the moiré bands with a large twist angle, $\theta = 2.88^\circ$. We see that there are a pair of linear bands (blue line) and a pairs of parabolic bands (red lines) around K_m , resulted from middle vdW layer. And, there are only two linear bands (red solid line) near E_f at either Γ (from top vdW layer) or K_b (from bottom vdW layer) points. When θ is reduced, the band width of the four moiré bands are narrowed, and the gap be-

tween flat bands and dispersive bands becomes obvious, see Fig. 3 (b). At the magic angle $\theta = 1.08^\circ$, the band width becomes nearly zero, and we get four degenerate MFBs, see Fig. 3 (c).

Here, the degeneracy of the four MFBs can be lifted by a perpendicular electric field as well, as shown in Fig. 3 (d), (e) and (f) with different θ and V . The outer two MFBs (blue lines) are isolated by the electric field, while the middle two (red) are still connected at K_m . We further calculate the valley Chern number of the four MFBs, as denoted in Fig. 3 (e) and (f). The valley Chern number depends on the electric field. When we increase V from 5 meV to 7 meV, a Chern number +1 is transferred from outer two MFBs to the central two.

The wave functions of the outer (inner) two MFBs are similar. Fig. 3 (g) gives the wave function of the 2nd MFB from bottom to up, while Fig. 3 (f) shows that of the top MFB. In the two situations, the wave function on the B sublattice of the middle graphene monolayer is always zero. Meanwhile, for the inner two bands, see Fig. 3 (g), rather large part of the wave function (about 53%) lies in the A sublattice of the middle graphene monolayer. As for the outer two MFBs, the corresponding value is only 18%.

Flat bands in (3+3+3)-DTFLG.—In the (1+3+1)-DTFLG cases above, we always get two pairs of MFBs at E_f gapped from other excited bands. If we use thicker FLG to build the DTFLG, we can introduce additional dispersive bands at E_f , coexisting with the two pairs of MFBs. As an example, in Fig. 4, we plot the moiré bands of (3+3+3)-DTFLG, where each vdW layer is a ABA-trilayer graphene. Fig. 4 (a), (c) are the alternating twisted configuration with $\theta = 2.88^\circ$ and $\theta = 1.08^\circ$, respectively. We see that there are eight bands at E_f , the band width of which are all narrowed with decreased θ . At the magic angle $\theta = 1.08^\circ$, we get not only two pairs of MFBs but also two pairs of linear bands with different Fermi velocity at K_{tb} . Fig. 4 (b), (d) are the chirally twisted configuration accordingly. At large θ , there are four bands at E_f , see Fig. 4 (b). But when decreasing θ , two additional bands quickly get close to the E_f near Γ and K_b , and at $\theta = 1.08^\circ$ the middle four bands becomes completely flat, see Fig. 4 (d).

Summary.—We have shown that a DTFLG, both the alternately and chirally twist situations, can have two pairs of MFBs at E_f , twice that of the magic angle TBG. Thus, it gives rise to a doubled DOS at E_f , which implies stronger correlation effects than all the known MHSs. Such MFBs in DTFLG are also topological non-trivial, and thus offers an promising platform to study the interplay between the correlation and band topology. A very notable issue is that the (1+3+1)-aDTFLG and (1+3+1)-cDTFLG has similar flat band structure but different crystal symmetry and MFB wave functions. So, an interesting question is that if such distinction (symmetry and wave functions) can lead to different correlation

phases. In experiment, double twisted trilayer graphene has already been fabricated very recently. Thus, we believe that our prediction can be readily tested in future experiment. Especially, we argue that the predicted two pairs of MFBs in DTFLG can be directly observed by the nanoAPRES technique.

We thank the supports by the National Natural Science Foundation of China (Grants No.11874160, 11534001, 11274129, 11874026 61405067), and the Fundamental Research Funds for the Central Universities (HUST: 2017KFYXJJ027), and NBRPC (Grants No. 2015CB921102).

* jinhua@hust.edu.cn

- [1] R. Bistritzer and A. H. MacDonald, *Proc. Natl. Acad. Sci.* **108**, 12233 (2011).
- [2] J. M. B. Lopes dos Santos, N. M. R. Peres, and A. H. Castro Neto, *Phys. Rev. Lett.* **99**, 256802 (2007).
- [3] J. M. B. Lopes dos Santos, N. M. R. Peres, and A. H. Castro Neto, *Phys. Rev. B* **86**, 155449 (2012).
- [4] Y. Cao, V. Fatemi, S. Fang, K. Watanabe, T. Taniguchi, E. Kaxiras, and P. Jarillo-Herrero, *Nature* **556**, 43 (2018).
- [5] Y. Cao, V. Fatemi, A. Demir, S. Fang, S. L. Tomarken, J. Y. Luo, J. D. Sanchez-Yamagishi, K. Watanabe, T. Taniguchi, E. Kaxiras, R. C. Ashoori, and P. Jarillo-Herrero, *Nature* **556**, 80 (2018).
- [6] Y. Jiang, X. Lai, K. Watanabe, T. Taniguchi, K. Haule, J. Mao, and E. Andrei, *Nature* **573**, 91 (2019).
- [7] M. Yankowitz, S. Chen, H. Polshyn, Y. Zhang, K. Watanabe, T. Taniguchi, D. Graf, A. F. Young, and C. R. Dean, *Science* **363**, 1059 (2019).
- [8] E. Codecido, Q. Wang, R. Koester, S. Che, H. Tian, R. Lv, S. Tran, K. Watanabe, T. Taniguchi, F. Zhang, M. Bockrath, and C. Lau, *Sci. Adv.* **5** (2019).
- [9] A. Kerelsky, L. J. McGilly, D. M. Kennes, L. Xian, M. Yankowitz, S. Chen, K. Watanabe, T. Taniguchi, J. Hone, C. Dean, A. Rubio, and A. N. Pasupathy, *Nature* **572**, 95 (2019).
- [10] M. Koshino, N. F. Q. Yuan, T. Koretsune, M. Ochi, K. Kuroki, and L. Fu, *Phys. Rev. X* **8**, 031087 (2018).
- [11] J. Kang and O. Vafek, *Phys. Rev. X* **8**, 031088 (2018).
- [12] Y.-H. Zhang, D. Mao, Y. Cao, P. Jarillo-Herrero, and T. Senthil, *Phys. Rev. B* **99**, 075127 (2019).
- [13] M. Koshino, *Phys. Rev. B* **99**, 235406 (2019).
- [14] N. R. Chebrolov, B. L. Chittari, and J. Jung, *Phys. Rev. B* **99**, 235417 (2019).
- [15] J. Y. Lee, E. Khalaf, S. Liu, X. Liu, Z. Hao, P. Kim, and A. Vishwanath, *Nat. Commun.* **10** (2019).
- [16] X. Liu, Z. Hao, E. Khalaf, J. Lee, Y. Ronen, H. Yoo, D. Najafabadi, K. Watanabe, T. Taniguchi, A. Vishwanath, and P. Kim, *Nature* **583**, 221 (2020).
- [17] Y. Cao, D. Rodan-Legrain, O. Rubies-Bigorda, J. M. Park, K. Watanabe, T. Taniguchi, and P. Jarillo-Herrero, *Nature* **583**, 215 (2020).
- [18] F. J. Culchac, R. B. Capaz, L. Chico, and E. Suarez Morell, [arXiv:1911.01347](https://arxiv.org/abs/1911.01347).
- [19] G. W. Burg, J. Zhu, T. Taniguchi, K. Watanabe, A. H. MacDonald, and E. Tutuc, *Phys. Rev. Lett.* **123**, 197702 (2019).

- (2019).
- [20] F. Wu and S. Das Sarma, *Phys. Rev. B* **101**, 155149 (2020).
- [21] R. Samajdar and M. S. Scheurer, *Phys. Rev. B* **102**, 064501 (2020).
- [22] F. Haddadi, Q. Wu, A. J. Kruchkov, and O. V. Yazyev, *Nano. Lett.* **20**, 2410 (2020).
- [23] C. Shen, Y. Chu, Q. Wu, N. Li, S. Wang, Y. Zhao, J. Tang, J. Liu, J. Tian, K. Watanabe, T. Taniguchi, R. Yang, Z. Y. Meng, D. Shi, O. V. Yazyev, and G. Zhang, *Nat. Phys* **16**, 520 (2020).
- [24] Z. Ma, S. Li, Y.-W. Zheng, M.-M. Xiao, H. Jiang, J.-H. Gao, and X. Xie, *Science Bulletin* **66**, 18 (2021).
- [25] S. Carr, C. Li, Z. Zhu, E. Kaxiras, S. Sachdev, and A. Kruchkov, *Nano. Lett.* **20**, 3030 (2020).
- [26] S. Chen, M. He, Y.-H. Zhang, V. Hsieh, Z. Fei, K. Watanabe, T. Taniguchi, D. H. Cobden, X. Xu, C. R. Dean, and M. Yankowitz, *Nat. Phys.* **17**, 374 (2021).
- [27] E. Suárez Morell, M. Pacheco, L. Chico, and L. Brey, *Phys. Rev. B* **87**, 125414 (2013).
- [28] S. Xu, M. M. Al Ezzi, N. Balakrishnan, A. Garcia-Ruiz, B. Tsim, C. Mullan, J. Barrier, N. Xin, B. A. Piot, T. Taniguchi, K. Watanabe, A. Carvalho, A. Mishchenko, A. K. Geim, V. I. Falko, S. Adam, A. H. C. Neto, K. S. Novoselov, and Y. Shi, *Nat. Phys.* (2021).
- [29] H. Polshyn, J. Zhu, M. Kumar, Y. Zhang, F. Yang, C. Tschirhart, M. Serlin, K. Watanabe, T. Taniguchi, A. MacDonald, *et al.*, *Nature* **588**, 66 (2020).
- [30] W.-J. Zuo, J.-B. Qiao, D.-L. Ma, L.-J. Yin, G. Sun, J.-Y. Zhang, L.-Y. Guan, and L. He, *Phys. Rev. B* **97**, 035440 (2018).
- [31] L. Rademaker, I. V. Protopopov, and D. A. Abanin, *Phys. Rev. Research* **2**, 033150 (2020).
- [32] J. Shin, B. Lingam Chittari, and J. Jung, (2021), [arXiv:2104.01570](https://arxiv.org/abs/2104.01570).
- [33] B. L. Chittari, G. Chen, Y. Zhang, F. Wang, and J. Jung, *Phys. Rev. Lett.* **122**, 016401 (2019).
- [34] G. Chen, L. Jiang, S. Wu, B. Lyu, H. Li, B. L. Chittari, K. Watanabe, T. Taniguchi, Z. Shi, J. Jung, Y. Zhang, and F. Wang, *Nat. Phys* **15**, 237 (2019).
- [35] G. Chen, A. Sharpe, P. Gallagher, I. Rosen, E. Fox, L. Jiang, B. Lyu, H. Li, K. Watanabe, T. Taniguchi, J. Jung, Z. Shi, D. Goldhaber-Gordon, Y. Zhang, and F. Wang, *Nature* **572**, 215 (2019).
- [36] Z. Ma, S. Li, M.-M. Xiao, Y.-W. Zheng, M. Lu, H. Liu, J.-H. Gao, and X. C. Xie, [arXiv:2001.07995](https://arxiv.org/abs/2001.07995).
- [37] S. Zhang, B. Xie, Q. Wu, J. Liu, and O. V. Yazyev, (2020), [arXiv:2012.11964](https://arxiv.org/abs/2012.11964).
- [38] J. Liu, Z. Ma, J. Gao, and X. Dai, *Phys. Rev. X* **9**, 031021 (2019).
- [39] F. Wu, T. Lovorn, E. Tutuc, I. Martin, and A. H. MacDonald, *Phys. Rev. Lett.* **122**, 086402 (2019).
- [40] M. Serlin, C. L. Tschirhart, H. Polshyn, Y. Zhang, J. Zhu, K. Watanabe, T. Taniguchi, L. Balents, and A. F. Young, *Science* **367**, 900 (2020).
- [41] X. Lu, P. Stepanov, W. Yang, M. Xie, M. Aamir, I. Das, C. Urgell, K. Watanabe, T. Taniguchi, G. Zhang, A. Bachtold, A. MacDonald, and D. Efetov, *Nature* **574**, 653 (2019).
- [42] A. Sharpe, E. Fox, A. Barnard, J. Finney, K. Watanabe, T. Taniguchi, M. Kastner, and D. Goldhaber-Gordon, *Science* **365**, 605 (2019).
- [43] E. Khalaf, A. J. Kruchkov, G. Tarnopolsky, and A. Vishwanath, *Phys. Rev. B* **100**, 085109 (2019).
- [44] X. Li, F. Wu, and A. H. MacDonald, [arXiv:1907.12338](https://arxiv.org/abs/1907.12338).
- [45] C. Mora, N. Regnault, and B. A. Bernevig, *Phys. Rev. Lett.* **123**, 026402 (2019).
- [46] Z. Zhu, S. Carr, D. Massatt, M. Luskin, and E. Kaxiras, *Phys. Rev. Lett.* **125**, 116404 (2020).
- [47] G. A. Tritsarlis, S. Carr, Z. Zhu, Y. Xie, S. B. Torrisi, J. Tang, M. Mattheakis, D. T. Larson, and E. Kaxiras, *2D Mater.* **7**, 35028 (2020).
- [48] G. A. Tritsarlis, Y. Xie, A. M. Rush, S. Carr, M. Mattheakis, and E. Kaxiras, *J. Chem. Inf. Model.* **60**, 3457 (2020).
- [49] Z. Zhu, P. Cazeaux, M. Luskin, and E. Kaxiras, *Phys. Rev. B* **101**, 224107 (2020).
- [50] F. Wu, R.-X. Zhang, and S. Das Sarma, *Phys. Rev. Research* **2**, 022010 (2020).
- [51] Z. Zhu, S. Carr, D. Massatt, M. Luskin, and E. Kaxiras, *Phys. Rev. Lett.* **125**, 116404 (2020).
- [52] T. Cea, N. R. Walet, and F. Guinea, *Nano. Lett.* **19**, 8683 (2019).
- [53] S. Carr, C. Li, Z. Zhu, E. Kaxiras, S. Sachdev, and A. Kruchkov, *Nano. Lett.* **20**, 3030 (2020).
- [54] K.-T. Tsai, X. Zhang, Z. Zhu, Y. Luo, S. Carr, M. Luskin, E. Kaxiras, and K. Wang, (2019), [arXiv:1912.03375](https://arxiv.org/abs/1912.03375).
- [55] J. M. Park, Y. Cao, K. Watanabe, T. Taniguchi, and P. Jarillo-Herrero, *Nature* **590**, 249 (2021).